Mater. Res. Soc. Symp. Proc. Vol. 1773 © 2015 Materials Research Society
DOI: 10.1557/opl.2015.522

Exploring the Role of Phosphate Structural Distortions on the Sodium Jump Dynamics in NASICON Phases

Todd M. Alam[*,1] Nelson Bell,[2] Jill Wheeler,[2] Erik D. Spoerke,[2] Randall T. Cygan,[3] and David Ingersoll[4]
[1]Department of Organic Material Science, [2]Department of Electronic, Optical and Nanostructure Materials, [3]Department of Geoscience Research and Application, [4]Department of Power Sources Research and Development, Sandia National Laboratories, Albuquerque, NM 87185 USA

ABSTRACT

High temperature solid state sodium (^{23}Na) magic angle spinning (MAS) NMR spin lattice relaxation times (T_1) were evaluated for a series of NASICON ($Na_3Zr_2PSi_2O_{12}$) materials to directly determine Na jump rates. Simulations of the T_1 temperature variations that incorporated distributions in Na jump activation energies, or distribution of jump rates, improved the agreement with experiment. The ^{23}Na NMR T_1 relaxation results revealed that distributions in the Na dynamics were present for all of the NASICON materials investigated here. The ^{23}Na relaxation experiments also showed that small differences in material composition and/or changes in the processing conditions impacted the distributions in the Na dynamics. The extent of the distribution was related to the presence of a disordered or glassy phosphate phase present in these different sol-gel processed materials. The ^{23}Na NMR T_1 relaxation experiments are a powerful tool to directly probing Na jump dynamics and provide additional molecular level details that could impact transport phenomena.

INTRODUCTION

Sodium ion conducting solids continue to be explored for future electrochemical energy storage applications [1]. In particular, Sodium Super Ionic Conductor (NASICON) materials are being actively pursued due to their known high ionic conductivity [2]. The conductivity of NASICON-type materials is directly proportional to the Na^+ carrier mobility (Na jumps), and is typically described as being modulated by structural restrictions along the conduction pathway, which is commonly referred to as the "bottleneck" region. It has been shown that for a NASICON-type structures that contain cations of different sizes, the PO_4 tetrahedra that bridge/link the ZrO_6 octahedra are distorted. These local PO_4 environments and distortions are not always clearly identified using XRD, yet differences in micro-structure and the presence of disordered or glassy phases influence the Na conductivity [3]. Experimental techniques that measure both the local molecular-level Na jump-motions and the local Na structural environment would provide additional insight into the role of structural distortions and phase impurities on the observed NASICON conductivity. In this paper, high temperature ^{23}Na NMR spin lattice relaxation (T_1) experiments will be presented, along with how the Na jump rates between different cation lattice sites and the corresponding activation energies were measured. It was found that for compositions near the optimal conductive $Na_3Zr_2PSi_2O_{12}$ stoichiometry that slight changes in the synthesis and processing conditions produced variations in the Na jump rates along with changes in the dynamic distributions.

EXPERIMENT

NMR Spectroscopy

All solid state high temperature ^{23}Na magic angle spinning (MAS) NMR spectra were collected on a Bruker Avance I 400 MHz spectrometer, operating 105.8 MHz for ^{23}Na using a 7 mm DOTY Scientific (Columbia, SC) DPI 7 mm probe spinning at 4 kHz. A standard inversion recovery pulse sequence was used to determine the spin-lattice relaxation time (T_1), with 32 inter-pulse relation delays and 8 to 16 scan averages. Recovery curves were analyzed using the Bruker Biospin TOPSIN software package. The sample temperatures were varied between 25 ^{o}C to 500 ^{o}C, and were previously calibrated using the melting points of secondary external standards.

Materials Preparation

The $Na_{3.0}Zr_2PSi_2O_{12}$ materials were prepared as briefly described below. The chemical precursors included zirconium (IV) butoxide (nominally 80 wt% in 1-butanol, Sigma-Aldrich), acetyl acetone (Reagent Plus, >99%, Sigma-Aldrich), tetraethyl orthosilicate (TEOS, >99%, Aldrich), sodium acetate, sodium phosphate tribasic dodecahydrate (Na_3PO_4•$12H_2O$, >98%, Sigma-Aldrich), NaOH, and pyrophosphoric acid. Deionized (DI) water (Millipore Synergy, 18.2 MΩ resistivity) and isopropanol (Cleanroom LP grade) were used as solvents. Adjustments to the pH were performed using 1.0 N HNO_3 (Sigma-Aldrich) and 1.0 N NH_4OH (Sigma-Aldrich). The Zr butoxide solution was assayed gravimetrically for true Zr concentration (86.3 wt%), with this determined concentration being used with the molar stoichiometry for subsequent powder precipitation. DI H_2O was used to dissolve Na_3PO_4•$12H_2O$ and sodium acetate in a Teflon beaker, with pH adjustment to 11.8 using concentrated HNO_3. Once all solids were dissolved, TEOS was added to the reaction vessel as a phase separated liquid, followed by strong vortex agitation. After 90 minutes, the TEOS reacted to create an opaque white precipitate. A solution of Zr butoxide and acetylacetone was diluted in isopropanol with the addition of acetylacetone, creating a transparent, yellow solution. The Zr solution was added rapidly to the water, P, Si, and Na precursor solution, leading to precipitation of a white gel. Sonication with an ultrasonic probe (Branson Ultrasonics, 250 W) with a micro-tip for 5 minutes was used to mix and break up aggregates using 0.5 second on/off pulses at 50% power. After aging for 2 hours, the precipitate was placed in a rotovap, and solvent was removed until a thick cake was formed, followed by drying at 80 ^{o}C overnight. Full solvent removal required an additional period of solvent evaporation under vacuum (> 20 in Hg) in a vacuum oven set to 75^{o}C for 3 days. To address the role of minor stoichiometry changes samples with a 1% and 2% excess in Na cation concentration were also prepared, and are denoted as $Na_{3.03}$ and $Na_{3.06}$ materials. The air dried gel powders from each composition were manually crushed, followed by calcination under flowing air (4.7 l/min) at 800°C for 12 hours. To address the role of additional thermal processing, samples were also prepared by treating the base 800 ^{o}C material at 1000, 1100 or 1250 ^{o}C for either 12 or 40 hrs. The commercial NASICON sample was obtained from Ceramatek Inc. (Salt Lake City, UT) and was used without additional preparation. This material was nominally $Na_3Zr_2PSi_2O_{12}$, but contains additional proprietary components as additives.

NMR Relaxation Analysis

The ^{23}Na NMR spin lattice relaxation times (T_1) are sensitive to jump dynamics that are on the order of the inverse of the NMR Larmor observed frequency (ω_0) and are inversely related to the spin-lattice relaxation rates (R_1):

$$R_1 = \frac{1}{T_1} = K_Q\left[J_1(\omega_0) + 4J_2(2\omega_0)\right] \tag{1}$$

where K_Q is a measure of the mean squared coupling of the ^{23}Na quadrupolar electrical field gradient interaction and $J_n(n\omega_0)$ are the spectral densities describing the dynamics occurring. The simplest spectral density describes a random motion containing only a single jump rate (k) or correlation time τ_c (=1/k), and was introduced for NMR relaxation studies by Bloembergen, Purcell and Pound (BPP) [4],

$$J_n(n\omega_0) = \frac{2\tau_c}{1+(n\omega_0\tau_c)^2} \tag{2}$$

For a thermally activated ionic jump it is assumed that the correlation times follow the Arrhenius law via

$$\tau_c = \tau_0 \exp(E_a / k_B T) \tag{3}$$

where E_a is the activation energy for the jump process. There are several different ways to address dynamic distributions that may be revealed in the current T_1 relaxation studies. A distribution in the activation energies probabilities $P(E_a)$ can be assumed, with the observed NMR T_1 relaxation being an weighted average over individual (BPP) spectral densities

$$R_1 = \frac{1}{T_1} = K_Q\int_0^\infty P(E_a)\left[J_1(\omega_0) + 4J_2(2\omega_0)\right]dE_a \tag{4}$$

In the present study, a Gaussian distribution around the average activation energy E_a^0 with a half width distribution σ_a was assumed

$$P(E_a) = 1/\left(\sigma_a\sqrt{2\pi}\right)\exp\left[-\left(E_a - E_a^0\right)^2 / 2\sigma_a^2\right] \tag{5}$$

It is also possible to approach the modeling of the observed ^{23}Na relaxation by incorporating distributions in k (or τ_c). The Cole-Davidson (CD) spectral densities [5] have been used in a range of different ionic solid studies, and were also used to model the T_1 NMR relaxation,

$$J_{CD}(n\omega_0) = \frac{2\sin\left[\beta_{CD}\arctan\left(n\omega_0\tau_{CD}\right)\right]}{n\omega_0\left[1+\left(n\omega_0\tau_{CD}\right)^2\right]^{\beta_{CD}/2}} \quad (6)$$

where τ_{CD} represents the upper cutoff correlation time (= $1/k_{CD}$) for the Na jump, while β_{CD} describes a stretch parameter. The cut-off correlation time τ_{CD} was assumed to follow Arrhenius temperature behavior. From the distribution of correlation times in the CD spectral density a distribution of activation energies can be directly determined via Equation. 4.

DISCUSSION

As an example, the temperature variation of the ^{23}Na NMR T_1 relaxation for the Ceramatek NASICON sample is shown in Figure 1. For the Ceramatek sample (along with all of the additional $Na_{3.0}$, $Na_{3.03}$ and $Na_{3.06}$ materials) the NMR T_1 relaxation times revealed a minimum within the temperature range investigated. The appearance of this fast Na relaxation (short T_1) occurs due to Na jump correlation times matching the Larmor observe frequency at τ_c ~ 1.5 ns (*i.e.* at $\omega_0\tau_c \sim 1$) or equivalently the jump rate at $k \sim 6 \times 10^8$ (rad s^{-1}).

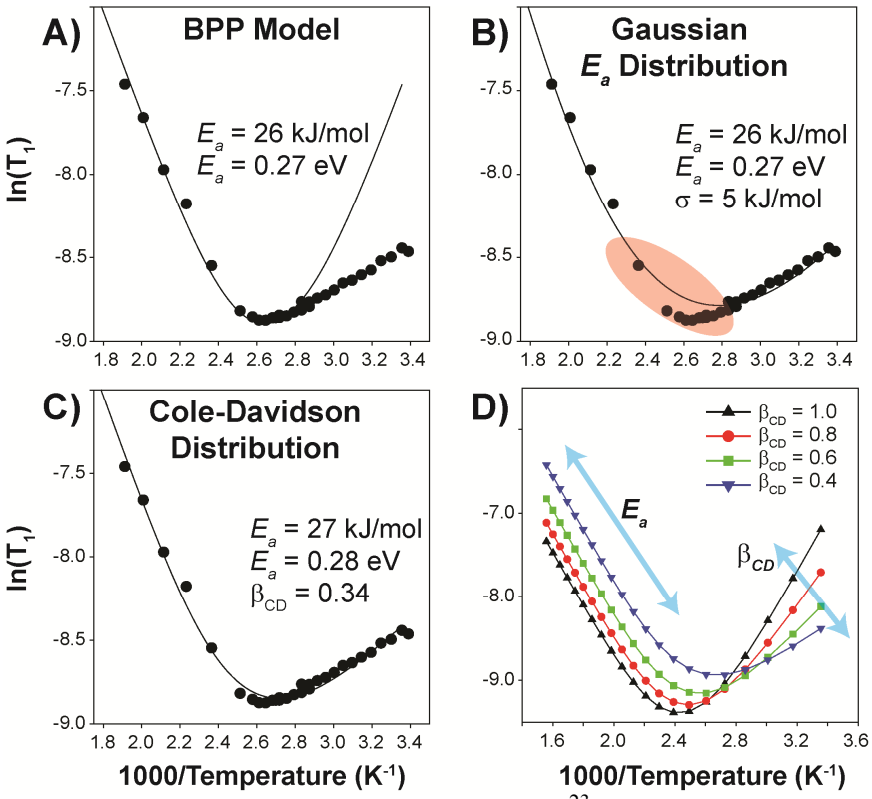

Figure 1. Predicted (lines) and experimental (symbols) of ^{23}Na NMR T_1 relaxation temperature dependence employing different Na jump models: A) The BPP description containing a single Na jump rate, B) A Gaussian distribution of Na jump activation energies, and C) A Cole-Davidson (CD) distribution of Na jump rates. D) The impact of the stretch parameter β_{CD} in the Cole-Davidson model on the predicted T_1 relaxation curves.

Modeling of the T_1 temperature dependence was useful in identifying the presence of Na jump rate distributions in the different NASICON samples. For example, Figure 1A shows the T_1's that would be observed if only one correlation time (or equivalently one jump rate or activation energy) were present using the BPP model (Equation 2). A symmetric temperature variation around the T_1 minimum is predicted and clearly does not match the experimentally observed ^{23}Na T_1 results. The reduction of the T_1 slope on the low temperature side is a known signature of distributions in τ_c (or equivalently E_a). Models assuming a Gaussian distribution (using Equation 5) were able to reproduce the reduction in T_1 slope as shown in Figure 1B. Small discrepancies between experiment and the Gaussian model were still observed near the T_1 minimum (shaded area), and have previously been argued to result from non-Gaussian distributions in E_a. A model that incorporated a Cole-Davidson (CD) distribution and spectral density (Equation 6) reproduced both the differences in the high and low temperature variations in the ^{23}Na NMR T_1 relaxation curve, and for this sample improved the fit near the T_1 minimum (Figure 1C). The impact of the stretch parameter β_{CD} in the CD spectral density is evaluated in Figure 1D, and shows that as β_{CD} decreases the slope on the low temperature side of the minimum is reduced, while the slope of the high temperature region remains constant and is proportional to E_a. This reduced T_1 slope arises from the presence of smaller E_a components that have significant contribution to the ^{23}Na NMR relaxation at lower temperatures. The CD distribution model was used for the subsequent discussion of NASICON lot variation below.

Examples of the variation of the ^{23}Na NMR T_1 relaxation temperature behavior for different material compositions and processing conditions are shown in Figure 2. Increasing the Na concentration or the processing temperature/extent in the sol-gel process had minimal effect on E_a, but these sol-gel derived materials all have a lower E_a than measured in the commercial Ceramatek NASICON material.

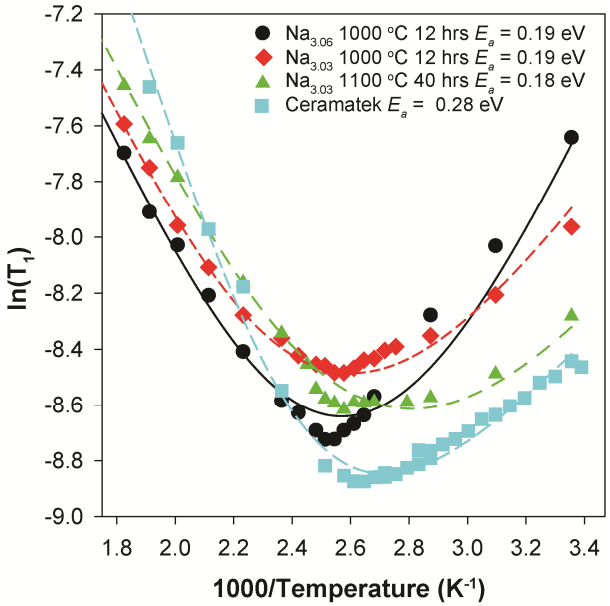

Figure 2. Temperature variation of the ^{23}Na NMR T_1 relaxation times (symbols) for different NASICON compositions and processing temperatures. Fits (lines) used the Cold-Davidson spectral density in Equation 6.

Increasing the Na concentration did decrease the size of the τ_c distribution in the $Na_{3.06}$ material with $\beta_{CD} \sim 1$ in comparison to the $Na_{3.03}$ composition, but increasing the extent of processing for $Na_{3.03}$ also produced an increase in the τ_c (or E_a) distribution. While the XRD results were invariant for the different sol-gel processed materials, the phosphorous (^{31}P) and sodium (^{23}Na) MAS NMR revealed large changes in the number and concentration of different local phosphate structures and sodium environments (MAS NMR results to be presented in detail elsewhere). The increasing concentration of different phosphate species correlates with larger distributions and reduced activation energies for the Na jump dynamics in these sol-gel produced NASICON materials.

CONCLUSIONS

The ^{23}Na NMR T_1 relaxation experiments presented here demonstrate that the rate of Na jumps and the activation energies can be directly determined in NASICON materials. The analysis of the complete T_1 temperature variation on both sides of the T_1 minimum also allowed a mapping of the Na dynamics including distributions in either the jump correlation times or activation energies. Changes in the Na concentration and processing temperature produced small, but distinct variations in the Na jump dynamic distributions. This information provides additional molecular level details that can be used to assess the impact of the synthetic preparation protocol on the final Na dynamics in NASICON.

ACKNOWLEDGMENTS

Sandia is a multi-program laboratory operated by Sandia Corporation, a Lockheed Martin Company, of the United States Department of Energy's National Nuclear Security Administration under Contract DE-AC04-94AL85000. This work was partially funded by the U.S. Department of Energy, Office of Electricity Delivery and Energy Reliability, Energy Storage Systems Program.

REFERENCES

1. F. Lalère, J. B. Leriche, M. Courty, S. Boulineau, V. Viallet, C. Masquelier and V. Seznec, *Journal of Power Sources* **247** (0), 975-980 (2014).
2. N. Anantharamulu, K. Koteswara Rao, G. Rambabu, B. Vijaya Kumar, V. Radha and M. Vithal, *J Mater Sci* **46** (9), 2821-2837 (2011).
3. R. O. Fuentes, F. M. Figueiredo, F. M. B. Marques and J. I. Franco, *Solid State Ionics* **140** (1–2), 173-179 (2001).
4. N. Bloembergen, E. M. Purcell and R. V. Pound, *Physical Review* **73** (7), 679-712 (1948).
5. P. A. Beckmann, *Physics Reports* **171** (3), 85-128 (1988).